Original Article

Construction and validation of a prognostic model of lncRNAs associated with RNA methylation in lung adenocarcinoma

Liren Zhang[1]^, Lei Yang[2], Xiaobo Chen[3], Qiubo Huang[3], Zhiqiang Ouyang[4], Ran Wang[5], Bingquan Xiang[6], Hong Lu[1], Wenjun Ren[1,7]^, Ping Wang[1]^

[1]Department of Thoracic Surgery, The Second Affiliated Hospital of Kunming Medical University, Kunming, China; [2]Department of Traditional Chinese Medicine Rehabilitation Medicine, The Affiliated Calmette Hospital of Kunming Medical University, The First People's Hospital of Kunming, Kunming, China; [3]First Department of Thoracic Surgery, The Third Affiliated Hospital of Kunming Medical University, Yunnan Cancer Hospital, Yunnan Cancer Center, Kunming, China; [4]Department of Radiology, Kunming Yan'an Hospital, Yan'an Hospital Affiliated to Kunming Medical University, Kunming, China; [5]Department of Epidemiology and Biostatistics, University of California Irvine, Irvine, USA; [6]Department of Intensive Care Unit, The Third Affiliated Hospital of Kunming Medical University, Yunnan Cancer Hospital, Yunnan Cancer Center, Kunming, China; [7]Department of Cardiovascular Surgery, The First People's Hospital of Yunnan Province, The Affiliated Hospital of Kunming University of Science and Technology, Kunming, China

Contributions: (I) Conception and design: P Wang, W Ren; (II) Administrative support: P Wang; (III) Provision of study materials or patients: P Wang, W Ren; (IV) Collection and assembly of data: L Yang, X Chen; (V) Data analysis and interpretation: L Zhang, Z Ouyang, R Wang; (VI) Manuscript writing: All authors; (VII) Final approval of manuscript: All authors.

Correspondence to: Ping Wang, MD. Department of Thoracic Surgery, The Second Affiliated Hospital of Kunming Medical University, 374 Dianmian Street, Kunming 650101, China. Email: wangping2467@126.com; Wenjun Ren, MD. Department of Cardiovascular Surgery, The First People's Hospital of Yunnan Province, The Affiliated Hospital of Kunming University of Science and Technology, 157 Jinbi Road, Kunming 650118, China; Department of Thoracic Surgery, The Second Affiliated Hospital of Kunming Medical University, Kunming, China. Email: renwenjun_hx@163.com.

Background: Lung adenocarcinoma (LUAD) is a common type of lung cancer and one of the leading causes of cancer death worldwide. Long non-coding RNAs (lncRNAs) play a crucial role in tumors. The purpose of this study was to explore the expression of lncRNAs associated with RNA methylation modification and their prognostic value in LUAD.

Methods: The RNA sequencing and clinical data were downloaded from The Cancer Genome Atlas dataset, and the messenger RNA and lncRNAs were annotated by Ensemble. The lncRNAs related to RNA methylation regulators (RMlncRNAs) were filtered by Pearson correlation analysis between differentially expressed lncRNAs and RNA methylation regulators. Univariate Cox regression analysis, multivariate Cox regression analysis, and least absolute shrinkage and selection operator regression analysis were used to construct a prognostic model. The receiver operating characteristic curve (ROC) was plotted to validate the predictive value of the prognostic model. Then, tumor mutational burden (TMB) and microsatellite instability were used to compare the immunotherapy response. Finally, to perform a drug sensitivity analysis, the half-maximal inhibitory concentration (IC_{50}) of targeted drugs was calculated using pRRophetic package.

Results: In total, 18 RMlncRNAs associated with the prognosis of LUAD patients were identified. Then, six feature lncRNAs (*NFYC-AS1*, *OGFRP1*, *MIR4435-2HG*, *TDRKH-AS1*, *DANCR*, and *TMPO-AS1*) were used to construct a prognostic model. The ROC curves for training, testing, and validation sets showed that the prognosis model was effective. The subindex based on the prognostic model had a high correlation with TMB. The high-risk group might be subject to greater immune resistance according to the comparison of Tumor Immune Dysfunction and Exclusion scores. Finally, the IC_{50} of 11 drugs had differences between high- and low-risk group, and only three of the drug's target genes (*ERBB4*, *CASP8*, and *CD86*) were differentially expressed.

Conclusions: In conclusion, a prognostic model based on six feature lncRNAs (*NFYC-AS1*, *OGFRP1*,

^ ORCID: Liren Zhang, 0009-0001-7644-9010; Ping Wang, 0009-0003-1618-262X; Wenjun Ren, 0000-0002-9748-2960.

MIR4435-2HG, *TDRKH-AS1*, *DANCR*, and *TMPO-AS1*) was constructed by bioinformatics analysis, which might provide a new insight into the evaluation and treatment of LUAD.

Keywords: Long non-coding RNAs (lncRNAs); RNA methylation regulators; prognostic model; immunotherapy response

Submitted Jun 27, 2024. Accepted for publication Jan 09, 2025. Published online Feb 24, 2025.
doi: 10.21037/tcr-24-1085
View this article at: https://dx.doi.org/10.21037/tcr-24-1085

Introduction

Lung cancer (LC) is currently the second leading cause of cancer worldwide and one of the main causes of high cancer mortality worldwide, lung adenocarcinoma (LUAD) is one of its major subtypes (1,2). In recent years, a large number of genomic studies have elucidated the complex molecular patterns of lung tumors, and targeted therapies for LUAD have been developed and applied. Study has shown that *KLF5* can promote cell proliferation and migration of LUAD by upregulating *STK24* (3). *STK24* may also be involved in the immune regulation process of LUAD (3). A novel circular RNA (circRNA) (circ_0004140), which originates from the oncogene *YAP1*, is found to be elevated in LUAD. The high levels of circ_0004140 correlate with poor outcomes and dysfunction of cytotoxic T lymphocytes (CTLs) in LUAD patients. Silencing circ_0004140 can influence the proliferation, migration, and apoptosis of LUAD cells. Moreover, increased expression of circ_0004140 is associated with cytotoxic lymphocyte depletion, while C-021 (*CCL22/CCR4* axis inhibitor) combined with anti-programmed cell death protein 1 (anti-PD-1) therapy can attenuate the development of LUAD and immune resistance (4). Currently, some of the latest treatment methods, including targeted drugs and immunotherapy drugs, are based on the results of LC gene research (5). With the widespread application of these treatments, patients' disease-free survival has been improved (6). However, the 5-year survival rate of patients remains low, at about 16.6% (7). Constructing risk diagnostic models and developing new tumor markers can help optimize treatment strategies for patients and improve treatment prognosis.

RNA methylation is considered a crucial process in epigenetic regulation, and occurs in both messenger RNA (mRNA) and long non-coding RNA (lncRNA) (8). Different methylation sites exhibit various forms of RNA methylation, including N1-methyladenosine (m1A), 5-methylcytosine (m5C), N6-methyladenosine (m6A), 7-methylguanosine (m7G), and 2-O-dimethyladenosine (m6Am) (9). RNA methylation plays a role in numerous physiological and pathological processes, and its improper regulation is strongly linked to the occurrence and progression of human cancers. In eukaryotic organisms, m6A methylation is the most widely used mRNA modification. It involves a fundamental process with m6A addition by methyltransferases, removal by demethylases, and identification by specific recognition molecules. Through these interactions, m6A plays a crucial role in regulating RNA metabolism and can influence target gene expression patterns and modulate physiological

Highlight box

Key findings

- We identified a signature of six RNA methylation-related long non-coding RNAs (lncRNAs) (*NFYC-AS1*, *OGFRP1*, *MIR4435-2HG*, *TDRKH-AS1*, *DANCR*, and *TMPO-AS1*) that showed a good prognostic effect on the survival of lung adenocarcinoma (LUAD) patients.

What is known and what is new?

- LncRNA and RNA methylation are crucial in the development of LUAD, affecting gene expression and cancer progression. Current LUAD prediction models have limited accuracy.
- In this study, we used lncRNAs related to RNA methylation regulators (RMlncRNAs) to construct a prognostic model for LUAD patients and linked the model to immunotherapy response and drug sensitivity.

What is the implication, and what should change now?

- This model can serve as a reliable predictor of survival for LUAD patients, provide a reference for doctors in clinical decision-making, and provide new clues for the study of the mechanism of LUAD.
- Future actions include integrating the model into clinical practice for better LUAD prognosis and investigating the therapeutic roles of the identified lncRNAs in immune resistance.

functions like self-renewal, invasion, and proliferation (10). The mammalian target of rapamycin (mTOR) signaling pathway is a well-studied area in tumor investigation. Recent evidence has indicated a possible close link between mTOR signaling and m6A methylation in the regulation of tumor metabolism. By suppressing m6A methylation levels, the Wnt and phosphoinositide 3-kinase-protein kinase B (PI3K-Akt)-mTOR signaling pathways are potentially activated, accelerating cancer development. In contrast, upregulation of m6A methylation can counteract these molecular changes in gastric cancer, which suggests that the oncogenic phenotype and activation signals may be directly modulated by m6A-associated enzymes and not only by the target genes directly regulated by m6A methylation (11,12). Several studies have indicated that RNA methylation, m6A-related regulatory factor METTL3, exhibits elevated expression levels in various types of cancers such as gastric cancer (13), liver cancer (14), and colorectal cancer (15). The expression of most m5C and m1A regulators was significantly different between lung squamous cell carcinoma (LUSC) and normal samples, among which m5C regulators were associated with poor prognosis (16). The m5C-related factors regulate known tumor promoters such as heparin binding growth factor (HDGF), transforming growth factor beta (TGF-β), and Ras GTPase-activating protein-binding protein 1 (G3BP1), thereby shaping the tumor microenvironment suitable for cancer cell migration and metastasis (17). Additionally, RNA methylation also plays a role in tumor suppression processes; in hepatocellular carcinoma, decreased m6A modification levels of microRNA126 affect its competing endogenous RNA (ceRNA) function, thereby accelerating tumor progression (18). M7G regulators can affect the infiltration, maturation, and activation of T cells in the tumor immune microenvironment (TIME). Among these regulators, METTL1 and WDR4 are m7G methyltransferases that have been widely studied in the context of T cell biology (19,20). Research by Ma *et al.* demonstrates that METTL1/WDR4-mediated m7GtRNA modification promotes mRNA translation and LC progression (21).

Most lncRNAs played an active role in epigenetic modifications, transcription, and multiple regulatory levels, and affect tumor initiation, necrosis, apoptosis, proliferation, cell cycle, and metastasis (22). Recently, the connection between RNA methylation and lncRNAs in tumors has emerged as a prominent area of research. Sun *et al.* found that the m5C methylation of lncRNA H19 mediated by NSUN2 could facilitate the progression and expansion of hepatocellular carcinoma by altering its interaction with the oncogenic protein G3BP1 (23). In gastric cancer cells, the demethylase ALKBH5 reduces the stability of lncRNA TP53TG1 and downregulates its expression, thereby promoting gastric cancer cell proliferation, migration, and cell cycle progression (24).

However, there is currently no research on the four types of RNA methylation (m6A, m1A, m5C, m7G)-related lncRNAs in LUAD. This study innovatively focused on lncRNA related to RNA methylation modification, screened and explored the expression of lncRNAs related to RNA methylation regulators (RMlncRNAs) in LUAD and its prognostic value, providing a new perspective for understanding the function of lncRNA in LUAD, especially its association with RNA methylation, an important epigenetic modification mechanism. Through bioinformatics analysis, a prognostic model of lncRNA was successfully constructed, providing a new tool for the prognosis assessment of LUAD patients. In addition, the study also deeply analyzed the correlation between the model and tumor mutational burden (TMB), microsatellite instability (MSI), immune infiltration analysis, immunotherapy response, and conducted drug sensitivity analysis, comparing the half-inhibitory concentration of multiple drugs between different risk groups, providing an important basis for the personalized treatment of LUAD. We present this article in accordance with the TRIPOD reporting checklist (available at https://tcr.amegroups.com/article/view/10.21037/tcr-24-1085/rc).

Methods

Data source

The RNA sequencing (RNA-seq) and clinical data were extracted from The Cancer Genome Atlas (TCGA) database (https://www.cancer.gov/ccg/research/genome-sequencing/tcga), including 524 samples of LUAD and 59 normal controls (NCs). Subsequently, mRNA and lncRNA were annotated using Ensembl (https://asia.ensembl.org/index.html). The GSE31210 dataset was downloaded from the Gene Expression Omnibus (GEO) (https://www.ncbi.nlm.nih.gov/geo/) and used as a validation cohort. Previous studies have reported a total of 76 genes related to methylation (9,12,25-29) (Table S1). The study was conducted in accordance with the Declaration of Helsinki (as revised in 2013).

Differential expression and mutation analysis of RNA methylation regulators

RNA methylation regulators were obtained from recent literature. The LIMMA package (version 3.52.1) (|logFC| >1 and P<0.05) (30) was used to identify differentially expressed genes (DEGs) between LUAD and NC samples. The differentially expressed RNA methylation regulators were identified by overlapping DEGs and RNA methylation regulator screening. The MAFTOOLS package was used to create mutation profiles of methylation regulators that exhibit differential expression in LUAD patients (31). The RCircos package (32) was used to locate the copy number variations (CNVs) of methylation regulatory genes on chromosomes.

Differential expression analysis of lncRNA

Differential expression of lncRNA (DE-lncRNAs) was obtained using the LIMMA package (30). Pearson correlation analysis was performed to extract lncRNAs related to methylation regulatory factors that were differentially expressed [|Pearson correlation coefficient (R)| >0.5, P<0.001] and correlated with methylation regulatory factors.

Univariate Cox regression analysis, multivariate Cox regression analysis, and least absolute shrinkage and selection operator (LASSO) regression analysis

Univariate Cox regression analysis was used to screen RMlncRNAs associated with the prognosis of LUAD patients [P<0.05, | hazard ratio (HR) −1| >0.1]. LUAD patients were divided into training and validation sets at a 1:1 ratio, and then LASSO and multivariate Cox regression analysis were used to further screen for feature genes. Additionally, the survival package (version 3.2-7) was utilized to calculate the risk scores for the training, testing, and validation sets. Risk scores were calculated using the following algorithm:

$$\text{Risk score} = h0(t) * \exp(\beta 1X1 + \beta 2X2 + \ldots + \beta nXn) \quad [1]$$

Then, using the median risk scores, patients in the training, validation, and testing sets were categorized into high- and low-risk groups. The Survminer package (version 0.4.8) was used to plot Kaplan-Meier curves, comparing the survival rates between the high- and low-risk groups. To further evaluate the effectiveness of the prognostic model, TimeROC software (version 0.4) was used to plot the receiver operating characteristic (ROC) curve with a 5-year survival time node. Survival status and RMlnc score curves were plotted to validate the prognostic model. Additionally, the predictive model was validated on the testing and validation sets.

Subgroup analysis and nomogram construction

In subgroup analysis, the 177 samples with complete data from the TCGA-LUAD dataset were divided into different groups based on age, gender (male and female), stage (I, II, III, IV), pathological M (M0 or M1), pathological T (T1, T2, T3, T4), and pathological N (N0 or N1/N2). The expression levels of feature genes in different groups were analyzed. Stratified analysis was used to explore the correlation between different pathological features and risk scores. Then, single-factor and multi-factor Cox regression analyses were conducted to investigate whether the risk score was an independent prognostic factor. A nomogram was constructed based on the risk score and multivariable analysis to predict the possible 1-, 3-, and 5-year survival rates of LUAD patients. Finally, the performance of the nomogram was evaluated using calibration curves.

Principal component analysis (PCA) and immunotherapy response analysis

To further validate the prognostic value of lncRNAs, PCA was performed on RMlncRNAs from high- and low-risk groups using the Scatterplot3d package. Then, TMB and MSI were compared between high- and low-risk populations to assess the immunotherapy response. The impact of the prognostic model on immune heterogeneity was studied using the Tumor Immune Dysfunction and Exclusion (TIDE) model. In addition, the Cibersort algorithm was employed to perform immune infiltration analysis on the lncRNA profiles from the TCGA database, comparing disease groups (524 samples) with control groups (59 samples) to identify differential immune cells. Perform correlation analysis between differentially expressed immune cells and RMlncRNAs. The marker genes for 22 types of immune cells were obtained from a designated reference (table available at https://cdn.amegroups.cn/static/public/tcr-24-1085-1.xls).

Drug sensitivity analysis

The half-maximal inhibitory concentration (IC_{50}) of

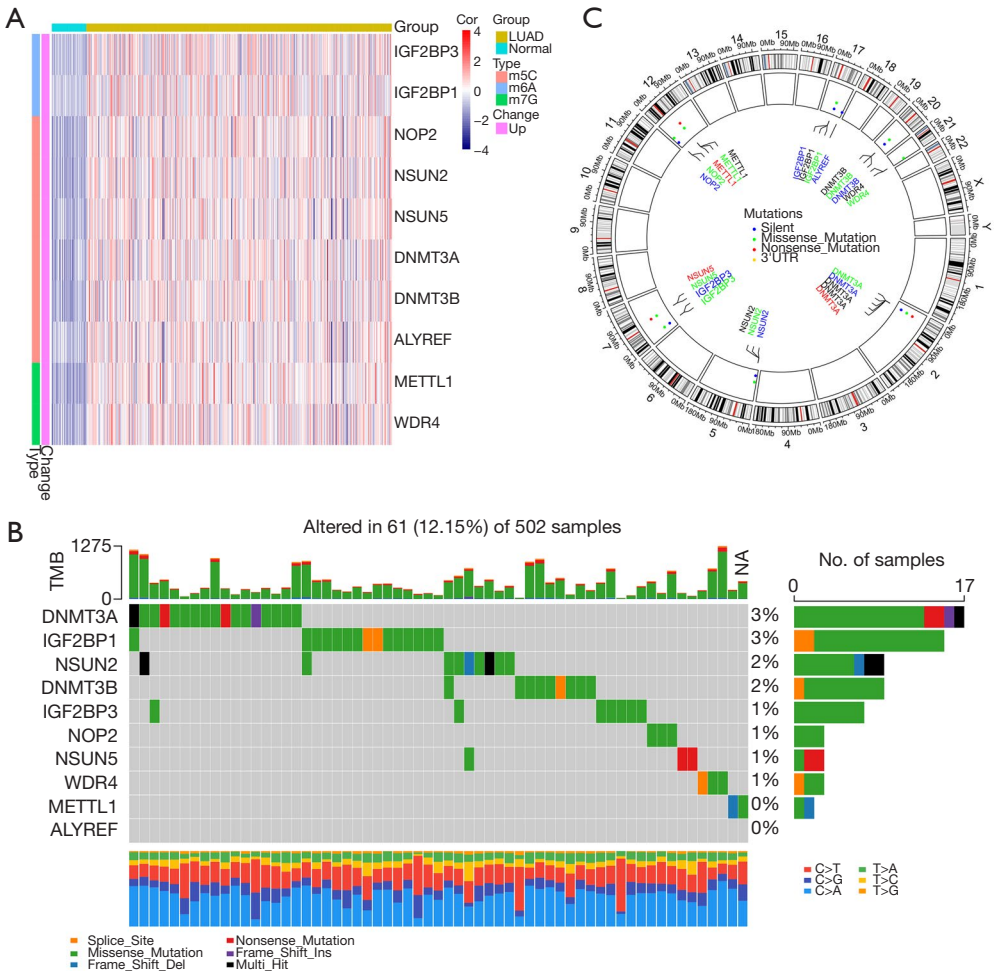

Figure 1 Differential expression and mutation analysis of RNA methylation regulatory factors in LUAD group compared to normal group. (A) Heatmap of differentially expressed RNA methylation regulatory factors. (B) Waterfall plot showing the somatic mutation frequency of differentially expressed RNA methylation regulatory factors. (C) CNV of methylation regulatory genes at chromosomal locations. TMB, tumor mutation burden; NA, no significance; CNV, copy number variation; LUAD, lung adenocarcinoma; UTR, untranslated region; Cor, correlation.

common chemotherapy drugs and molecular targeted drugs was calculated using the pRophetic package (33). The Wilcoxon test was employed to compare the IC_{50} of different drugs between high- and low-risk populations. The DrugBank database was utilized to obtain the target genes of drugs. Finally, the expression of target genes in the high- and low-risk populations of the training set was analyzed.

Statistical analysis

Sankey diagrams were generated using the giant package (34). Heatmaps were plotted using the pheatmap package (35). Kaplan-Meier analysis was performed to compare the survival differences between two groups of patients. A two-sided P<0.05 was considered statistically significant.

Results

A total of 10 differentially expressed RNA methylation regulators were identified in TCGA-LUAD

A total of 4,885 DEGs were detected between LUAD and NC samples, with 3,027 genes upregulated and 1,858 genes downregulated. Additionally, 10 differentially expressed RNA methylation regulators were identified, showing

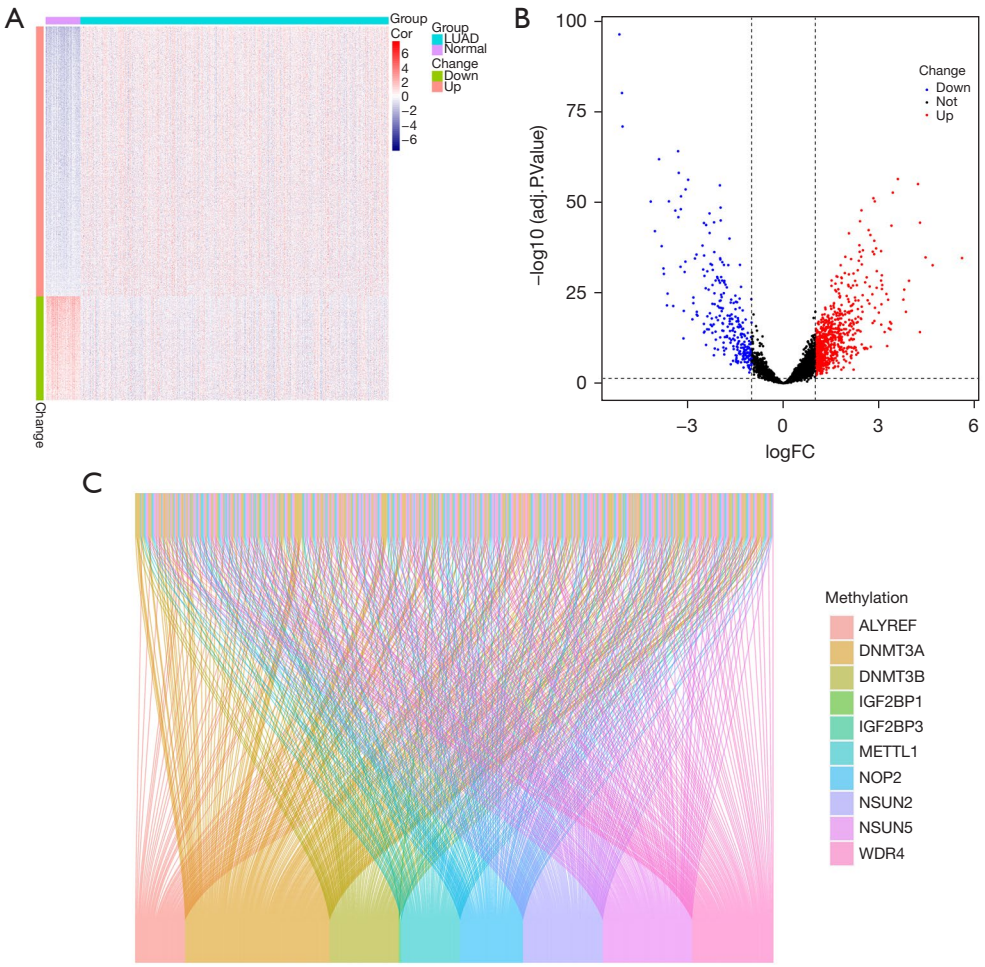

Figure 2 Identification of DE-lncRNAs in LUAD patients. (A,B) The heatmap and volcano plot illustrate the DE-lncRNAs between the lung adenocarcinoma group and the normal group. (C) Sankey diagram to illustrate the correlation between DE-lncRNAs and differentially expressed RNA methylation regulatory factors. DE-lncRNAs, differentially expressed long non-coding RNAs; LUAD, lung adenocarcinoma; FC, fold change; Cor, correlation.

high expression levels in LUAD samples (*Figure 1A*). The mutation frequency of differentially expressed RNA methylation regulators is shown in *Figure 1B*. The location variation of RNA methylation regulators on chromosomes due to CNVs is depicted in *Figure 1C*.

Identification of 233 DE-lncRNAs

A total of 986 lncRNAs were extracted from the TCGA-LUAD dataset, with 712 upregulated and 274 downregulated (*Figure 2A*,*2B*). A total of 233 DE-lncRNAs were identified. A Sankey diagram was generated based on the co-expression patterns of mRNA-lncRNA to illustrate the relationship between DE-lncRNAs and differentially expressed RNA methylation regulators (*Figure 2C*).

Construction and validation of prognostic model

A total of 18 RMlncRNAs associated with the prognosis of LUAD patients were selected (*Figure 3A*), including nine risk factors and nine protective factors (*Figure 3B*). Then, through LASSO and multivariate Cox regression analysis, six feature genes (*NFYC-AS1*, *OGFRP1*, *MIR4435-2HG*, *TDRKH-AS1*, *DANCR*, and *TMPO-AS1*) were identified (*Figure 3C*,*3D*). The overall survival (OS) curve showed statistically significant differences in survival rates between the high- and low-risk groups (P<0.001), with lower survival rates observed in the high-risk group (*Figure 3E*). The area

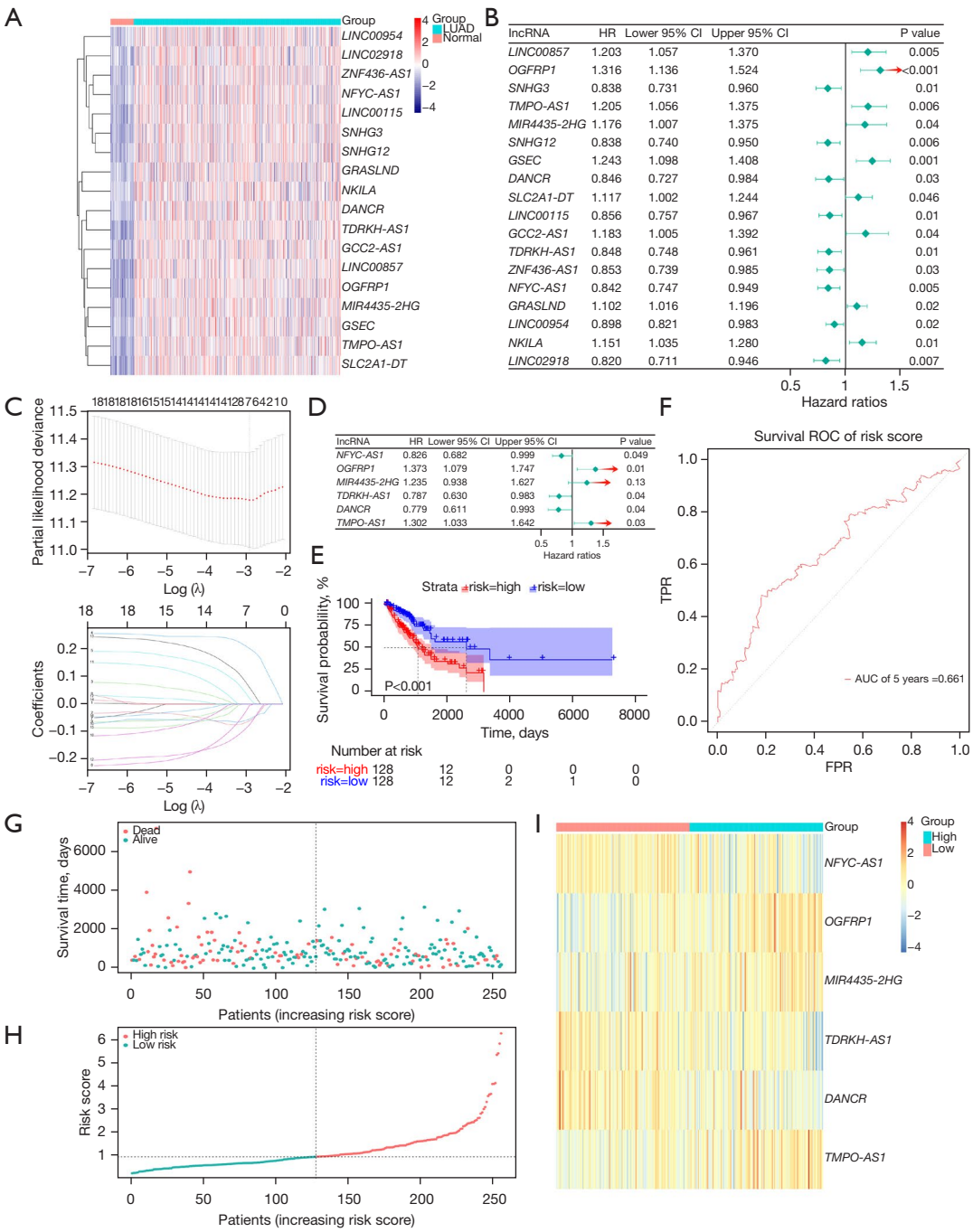

Figure 3 Construction and validation of the prognostic model. (A) Heatmap of the expression differences of 18 prognostic-related RMlncRNAs in the LUAD group and the normal group (blue represents low expression, red represents high expression). (B) Forest plot for univariate Cox regression analysis of RMlncRNAs. (C) LASSO regression analysis for feature gene selection. (D) Forest plot for multivariate Cox regression analysis of the six feature genes. (E) The Kaplan-Meier curve of the prognostic risk model shows that the overall survival rate in the high-risk group is lower than that in the low-risk group. (F) Determine the AUC of the prognostic risk model based on the ROC curve. (G-I) The distribution of risk scores in LUAD patients based on prognostic features, survival status, and the expression of RMlncRNAs. RMlncRNAs, lncRNAs related to RNA methylation regulators; LUAD, lung adenocarcinoma; LASSO, least absolute shrinkage and selection operator; ROC, receiver operating characteristic; lncRNA, long non-coding RNA; HR, hazard ratio; CI, confidence interval; TPR, true positive rate; FPR, false positive rate; AUC, area under the curve.

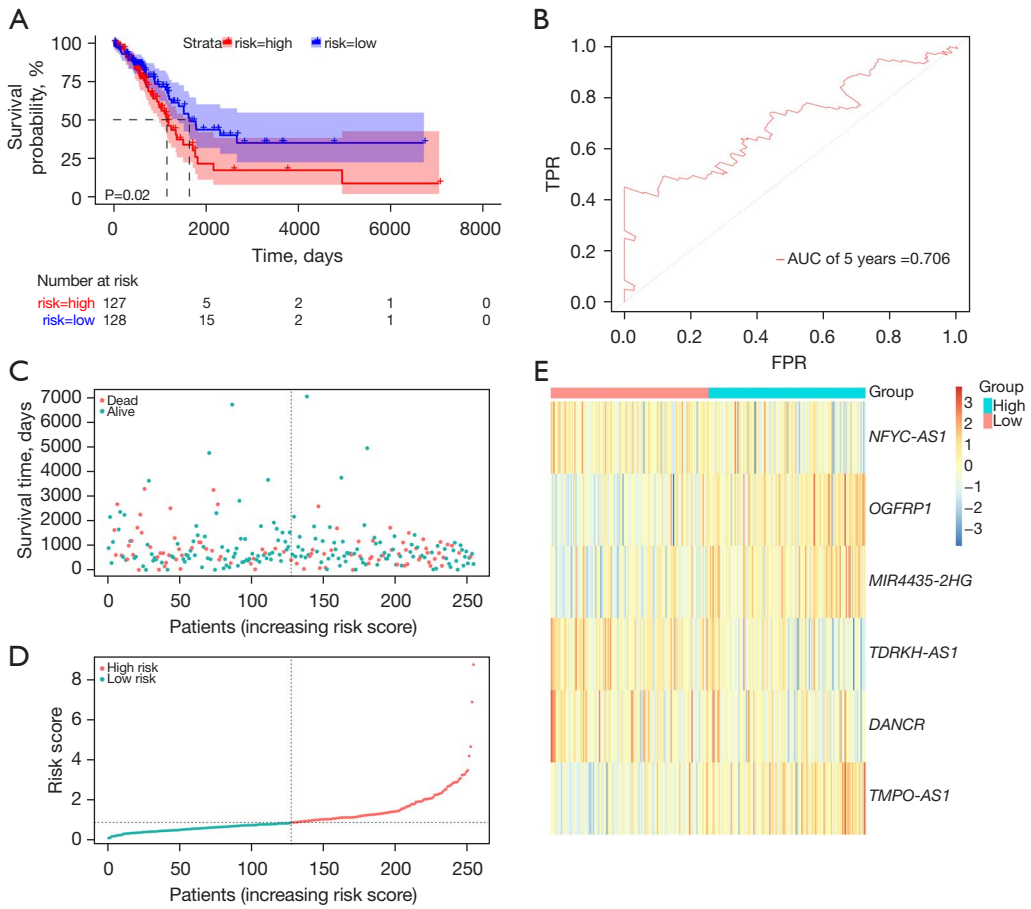

Figure 4 Prognostic value evaluation of the risk model in the test set. (A) The Kaplan-Meier curve shows that the overall survival rate is lower in the high-risk group than in the low-risk group. (B) Determine the AUC of the prognostic risk model based on the ROC curve. (C-E) Distribution of patient risk scores (based on prognostic features, survival status, and RMlncRNAs expression). RMlncRNAs, lncRNAs related to RNA methylation regulators; ROC, receiver operating characteristic; TPR, true positive rate; FPR, false positive rate; AUC, area under the curve.

under the curve (AUC) for predicting the 5-year survival rate of LUAD patients was 0.661, indicating good predictive performance of the model (*Figure 3F*). Additionally, patients with shorter survival times and censoring events were more abundant in the high-risk group (*Figure 3G,3H*). The heatmap showed high expression of *OGFRP1*, *MIR4435_2HG*, and *TMPO_AS1* in the high-risk group (HR >1) (*Figure 3I*). The results of the test and validation sets were consistent with the training set (*Figure 4A-4E*, Figure S1).

Risk score, pathological N, and pathological M were independent prognostic factors for LUAD

Comparison of the number of patients with different clinical features between the high- and low-risk groups showed no statistically significant differences (Table S2). Analysis of risk scores for different clinical features showed differences in stage and pathological N stage (*Figure 5A*). The expression analysis of feature genes in different clinical feature groups is shown in *Figure 5B*. Furthermore, significant differences were observed in the correlation between risk scores and different pathological features between the high- and low-risk groups (*Figure 5C*). Results of univariate and multivariate COX regression analysis showed that risk score, pathological N, and pathological M could serve as independent prognostic factors (*Figure 6A,6B*). The nomogram is presented in *Figure 6C*. The calibration curve of the nomogram indicated the effectiveness of the predictive model (*Figure 6D*).

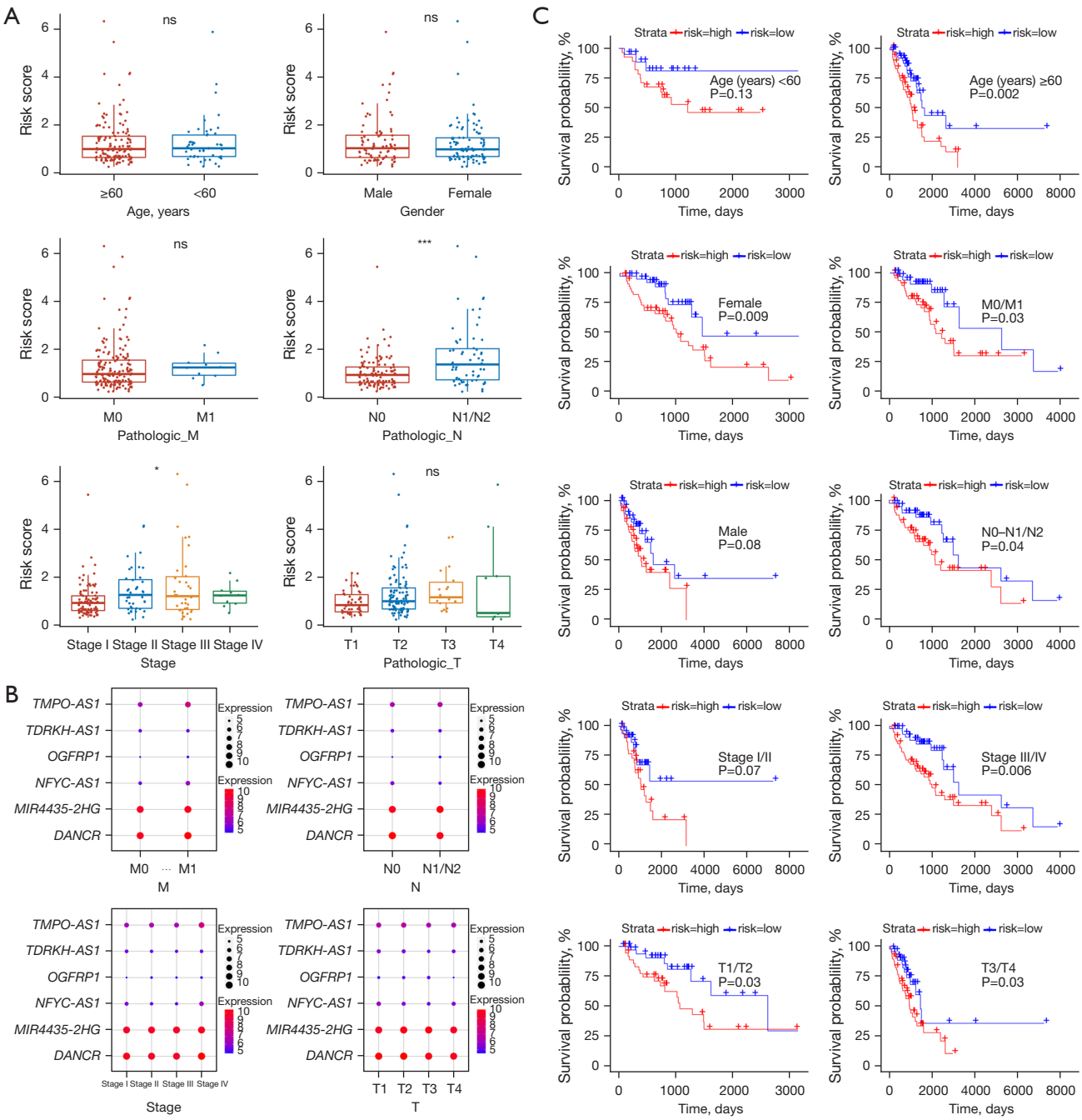

Figure 5 Comprehensive analysis of clinicopathologic features in relation to risk scores and gene expression. (A) Differences in risk scores among clinical and pathological features in different groups. (B) Expression of genes in the model across different clinical feature groups. (C) The Kaplan-Meier curve of stratified analysis exploring the correlation between risk score and different pathological features. ns, no significance; *, P<0.05; ***, P<0.001.

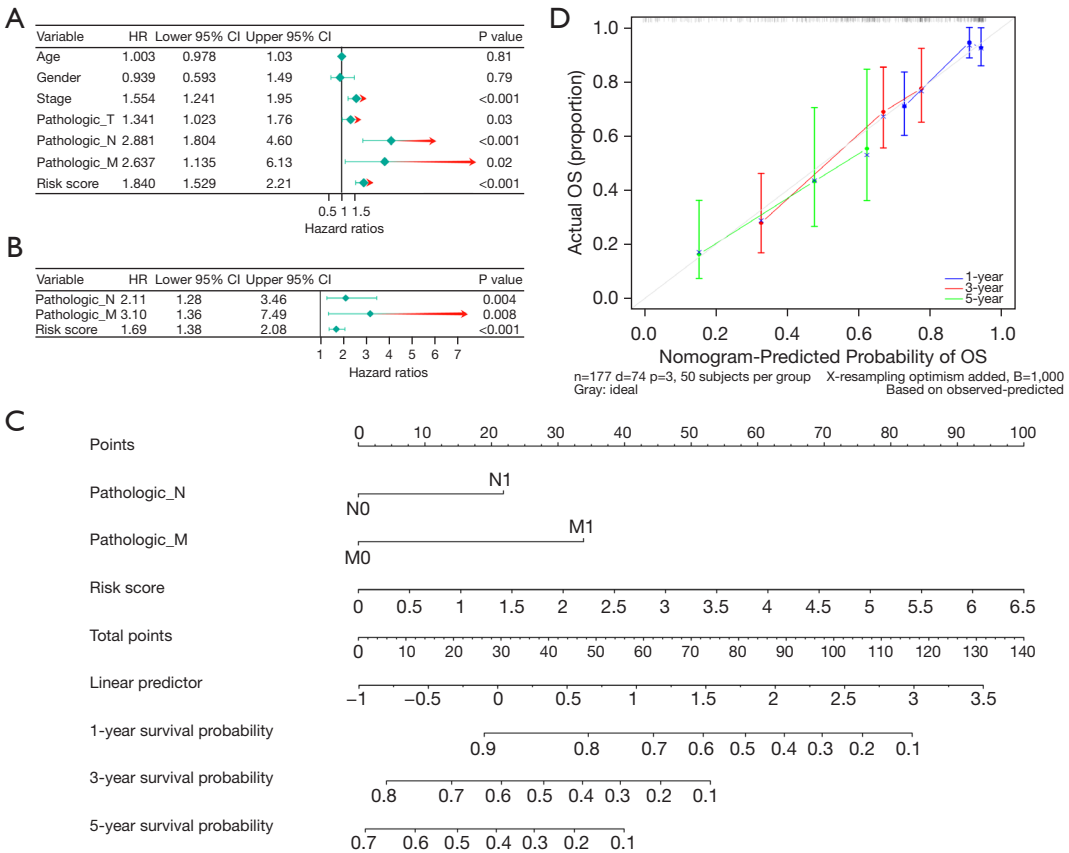

Figure 6 Correlation analysis of risk scores with clinical features and construction of prognostic model. (A) Forest plot for univariate Cox analysis of risk score and clinical features. (B) Forest plot for multivariate Cox analysis of risk score and clinical features. (C) Nomogram constructed based on the risk score. (D) Calibration curves for the risk score model at 1, 3, and 5 years. HR, hazard ratio; CI, confidence interval; OS, overall survival.

Differences in immunotherapy response between high- and low-risk groups

The results of principal component analysis indicated that samples could be distinctly classified into high- and low-risk groups based on characteristic lncRNAs (*Figure 7A*). Visualization results of somatic mutations in the high- and low-risk groups are shown in *Figure 7B*. *Figure 7C*,*7D* demonstrate significant differences in TMB and TIDE scores between the high- and low-risk groups. The high-risk group exhibited higher TMB compared to the low-risk group, suggesting a higher correlation between the subindex based on the prognostic model and TMB. Moreover, higher TIDE scores in the high-risk population suggest potentially greater immune resistance, indicating a higher potential for immune evasion and possibly poorer efficacy of immune checkpoint inhibitor (ICI) therapy. In addition, the expression results of the 22 types of immune cells in both the tumor and control groups revealed that B cells memory and Plasma cells were highly expressed in the tumor group (Figure S2A,S2B). Furthermore, with the exception of T cells CD4 naive, the expressions of the other 21 types of immune cells exhibited significant differences (P<0.001) between the tumor and control groups (Figure S2C). The correlation results between six RMlncRNAs (*NFYC-AS1*, *OGFRP1*, *MIR4435-2HG*, *TDRKH-AS1*, *DANCR*, *TMPO-AS1*) and the 21 types of immune cells are presented in Figure S2D.

The IC_{50} of 11 drugs was significant differences between high- and low-risk groups

Wilcoxon test revealed significant differences in IC_{50} values for 11 drugs (AICAR, BIBW2992, Bryostatin.1, EHT.1864, GDC0941, Gefitinib, JNK.Inhibitor.VIII, KU.55933,

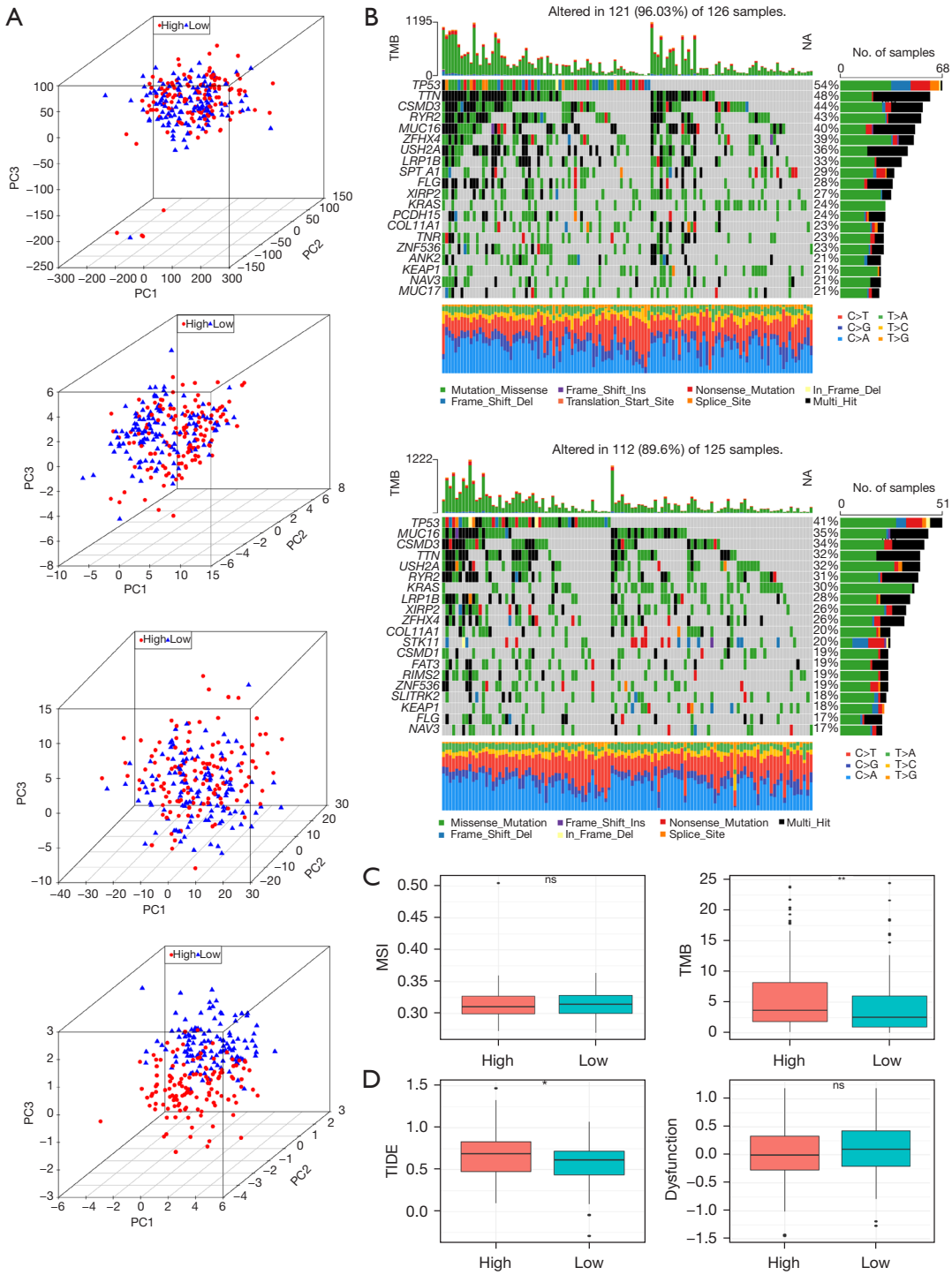

Figure 7 Study on the main component analysis of high and low risk groups and the difference of immune-related indexes based on multi-group characteristics. (A) Principal component analysis between the high- and low-risk groups based on entire gene expression profiles, RNA methylation related genes, RMlncRNAs, and risk model based on six RMlncRNAs. (B) Waterfall map of somatic mutation frequency between high and low risk groups. (C) Differences of TMB and MSI in high and low risk groups. (D) Differences of dysfunction and TIDE scores in high and low risk groups. ns, no significance; *, P<0.05; **, P<0.01. TMB, tumor mutation burden; NA, no significance; MSI, microsatellite instability; TIDE, Tumor Immune Dysfunction and Exclusion; PC, principal component; RMlncRNAs, long non-coding RNAs related to RNA methylation regulators.

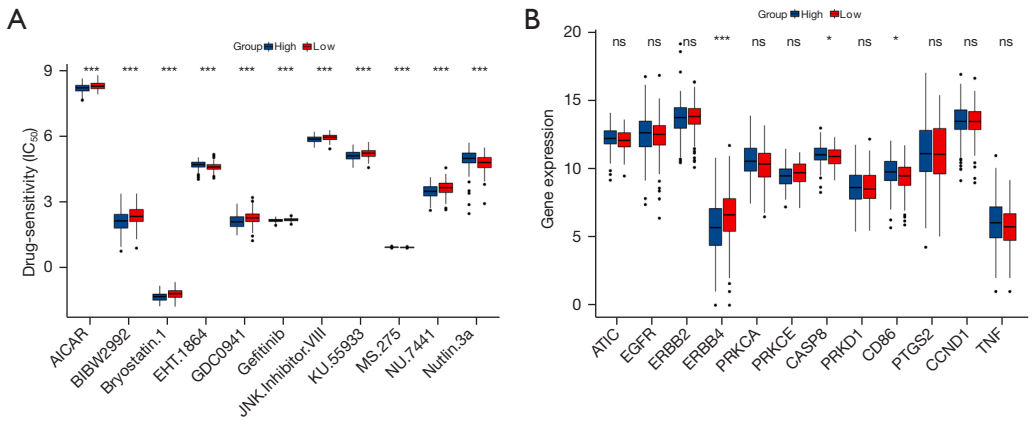

Figure 8 Analysis of differences in drug sensitivity and target gene expression between high and low risk groups. (A) Differences of drug sensitivity in high and low risk groups. (B) Differences of target genes in high and low risk groups. ns, no significance; *, P<0.05; ***, P<0.001. IC_{50}, the half-maximal inhibitory concentration.

MS.275, NU.7441, and Nutlin.3a) between the high- and low-risk groups (*Figure 8A*). Subsequently, 12 target genes corresponding to the drugs were obtained, among which only three (*ERBB4*, *CASP8*, and *CD86*) showed differences between the high- and low-risk groups (*Figure 8B*).

Discussion

As LC treatment methods continue to evolve, the application of predictive biomarkers has made significant progress (36). Due to the high heterogeneity of LUAD cells, there are still differences in treatment outcomes among patients with similar clinical characteristics and pathological presentations (37). In epigenetic modification, RNA methylation plays a crucial role in regulating gene expression and maintaining stability. For example, m6A methylation acts as a versatile checkpoint, that can couple different layers of gene regulation with one another (38). As research progresses, the close relationship between lncRNA and RNA methylation in tumor occurrence and development has been discovered. For instance, Chen *et al.* found that lncRNA lnc-H2AFV-1 alters m6A modification by modulating m6A methyltransferases METTL3/14 and FTO, mediating downstream target *IFT80* to promote the progression of head and neck squamous cell carcinoma (39). Wanna-Udom *et al.* discovered that METTL3 is crucial in TGF-β-induced epithelial-mesenchymal transition (EMT) in LC. It primarily functions by promoting m6A modification, elevating total mRNA levels, and enhancing the stability of JUNB mRNA, which is a key transcriptional regulator of EMT (40). The study also revealed that *YTHDF2* is overexpressed in LC tissues, facilitating the growth of LC cells. It directly interacts with the m6A modification site in the 3' untranslated region (UTR) of 6-phosphogluconate dehydrogenase (6PGD), thereby promoting the translation of 6PGD mRNA in LC cells and enhancing the pentose phosphate pathway (PPP), which is essential for tumor growth (41). Moreover, research has indicated that m6A-modified lncRNAs can influence various biological processes. The impact of m6A modification on lncRNAs may involve several regulatory mechanisms: on one hand, it can modulate lncRNA function by creating binding sites for m6A reader proteins or altering local RNA structures to facilitate the binding of RNA-binding proteins (RBPs). On the other hand, m6A modification may also affect the interaction between RNA and DNA, as well as specific DNA sites, by influencing the triple helix structure of lncRNA (12). Therefore, RMlncRNAs have the potential to serve as innovative molecular indicators and possible therapeutic targets in cancer treatment. Currently, there is no research published on the characteristics of RMlncRNAs as tumor prognostic indicators. This study constructed an LUAD prognostic risk model based on RNA methylation-related lncRNAs, providing new clues for subsequent mechanistic research.

We identified 4,885 RMlncRNAs from the TCGA dataset. Through LASSO and multiple-factor analysis, we finally determined six RMlncRNAs to construct a model for predicting the survival rate of LUAD patients. The results indicated that patients in the high-risk group had shorter OS times. The AUC of the 5-year ROC curves for the training, testing, and validation sets were all greater than

0.6, demonstrating the effectiveness of these RMlncRNAs features in predicting the prognosis of LUAD patients. The calculated risk score, lymph node metastasis, and distant metastasis based on these RMlncRNAs were independent prognostic factors for LUAD patients, playing a predictive role in the prognosis of LUAD.

This study screened lncRNAs related to RMlncRNAs by correlating DE-lncRNAs with RNA methylation regulatory factors. A prognostic risk model based on six RMlncRNAs (including *OGFRP1*, *MIR4435-2HG*, *TMPO-AS1*, *NFYC-AS1*, *TDRKH-AS1*, *DANCR*) was constructed. Some studies have already shown that these lncRNAs play roles in cancer. Opioid growth factor receptor pseudogene 1 (*OGFRP1*) has carcinogenic effects on non-small cell lung cancer (NSCLC), colorectal cancer (CRC), and gastric cancer (GC). *OGFRP1* regulates *LYPD3* expression through sponge miR-124-3p, promoting the progression of NSCLC (42). Dong *et al.*'s study found that *OGFRP1* promotes angiogenesis and EMT of CRC cells through the miR-423-5p/*CTCF* axis (43). Zhang *et al.* found that *OGFRP1* promotes GC progression by activating the AKT/mTOR pathway (44). MicroRNA4435-2 Host Gene (*MIR4435-2HG*) activates TGF-β signaling by sponge TGF-β1, promoting migration and proliferation of NSCLC (45). *MIR4435-2HG* promotes tumorigenesis by participating in six signaling pathways, including TGF-β, Wnt/β-catenin, MDM2/p53, PI3K/AKT, Hippo, and MAPK/ERK signaling pathways. It can competitively bind to multiple miRNAs to create a complex ceRNA network, thereby regulating the expression of downstream target genes. Elevated levels of *MIR4435-2HG* are strongly associated with clinical pathological features and poor prognosis in various tumors, making its high expression in peripheral blood or serum a valuable predictor of cancer risk. Additionally, *MIR4435-2HG* plays a role in the mechanisms of action for three anticancer drugs: resveratrol in LC, cisplatin in NSCLC and colon cancer, and carboplatin in triple-negative breast cancer (46).

As a lncRNA, *MIR4435-2HG* is also involved in the molecular cascade of other diseases such as coronary artery disease, osteonecrosis, osteoarthritis, osteoporosis and periodontitis. *MIR4435-2HG* exerts its functions through multiple mechanisms, including inhibiting cell apoptosis, adsorbing microRNAs (miRNAs), promoting cell proliferation, increasing cell invasion and migration ability, and enhancing EMT (47).

It shows diagnostic and prognostic value in various tumors and is considered a pan-cancer biomarker (48). Thymopoietin-antisense RNA 1 (*TMPO-AS1*) regulates the proliferation of LUAD cells by upregulating *SOX12* expression levels through sponge miR-326 (49). Qiu *et al.*'s study found that downregulation of TMPO-AS1 can induce apoptosis of LC cells by regulating the miR-143-3p/*CDK1* axis (50). Nuclear transcription factor Y subunit gamma-antisense RNA 1 (*NFYC-AS1*) is a commonly expressed nuclear antisense RNA, highly expressed in pan-cancer, controlling the cell cycle mitosis process (51). In LUAD, *NFYC-AS1* promotes the tumor cell proliferation, invasion, and apoptosis through autophagy, apoptosis, and MET/c-Myc oncogenic proteins (52). Furthermore, Tong *et al.*'s study found that the abnormal elevation of *NFYC-AS1* may promote the progression of LUAD through the autophagy-related gene *BIRC6* (53). In Ding *et al.*'s study, tudor and KH domain containing-antisense RNA 1 (*TDRKH-AS1*) acts as a sponge for miR-134-5p in breast cancer, thereby reducing the inhibitory effect of miR-134-5p on *CREB1* expression and exerting a tumor-promoting effect (54). In CRC, *TDRKH-AS1* promotes cancer cell proliferation and invasion through the β-catenin-activated Wnt signaling pathway (55). Its mechanism of action in LUAD remains to be further investigated. Differentiation antagonizing non-protein coding RNA (*DANCR*) was first discovered to be closely associated with the EMT process (56). *DANCR* is aberrantly expressed in various cancers and plays a key role in cancer cell proliferation, apoptosis, invasion, and drug resistance (57). LncRNA-DANCR promotes the progression of LUAD by regulating mTOR expression through sponge miR-496 (58). Besides miR-496, many other miRNAs have been verified as sponge targets for *DANCR* (59). The results of this study indicate that these six RMlncRNAs play important roles in the occurrence and prognosis of LUAD. However, there is currently no research on the potential significance of their association with RNA methylation in studying its relevance to the prognosis of LUAD patients.

In order to assess the practical clinical impact of the risk model, we also conducted an analysis of immune therapy response to evaluate the model's predictive ability for ICIs efficacy. TMB can reflect the ability and extent of tumor to generate new antibodies, and it has been shown to predict the efficacy of ICIs in multiple cancers (60). For NSCLC patients receiving ICIs treatment, TMB alone or in combination testing has good predictive ability (61,62). In the results of this study, the TMB of the high-risk group exceeded that of the low-risk group, indicating a high correlation between the risk model's classification index and TMB. The high-risk group is more likely to respond

to immune therapy compared to the low-risk group. The TIDE scores predict tumor immune escape capability by comprehensively assessing the activity of two immune evasion mechanisms. In this study, the predictive results of the TIDE scores indicated that patients in the high-risk group had better responses to immune therapy. Based on these results, we believe that this predictive model may provide a reference for the immune therapy efficacy in LUAD patients, and these RMlncRNAs may serve as new immune biomarkers in LUAD treatment.

Finally, we conducted drug sensitivity analysis. By analyzing 138 commonly used drugs, we identified 11 drugs with significant differences in sensitivity. Subsequently, we predicted their target genes and identified three target genes (*ERBB4*, *CASP8*, and *CD86*) that showed significant differences between the high- and low-risk groups. The corresponding drugs for these genes were afatinib (BIBW2992) and bryostatin-1. Afatinib is a kinase inhibitor approved for first-line treatment of metastatic NSCLC harboring non-resistant epidermal growth factor receptor (EGFR) mutations. It demonstrates greater activity and better tolerability than chemotherapy in patients with EGFR mutations (63). Bryostatin.1 is currently in the research stage and has potential value in the treatment of LUAD. Phase II clinical trials have been completed in combination with paclitaxel for stage IIIB, IV, or recurrent NSCLC patients (64). The model reflects the drug sensitivity of LUAD patients to these two drugs, providing a reference for drug selection in LUAD patients.

The model constructed in this study included the following lncRNAs: *NFYC-AS1*, *OGFRP1*, *MIR4435-2HG*, *TDRKH-AS1*, *DANCR*, *TMPO-AS1*, which may represent relevant biomarkers with potentially good predictive capabilities, holding significant implications for improving treatment outcomes and prognosis in patients with LUAD. This study still has some limitations. Firstly, it is a retrospective study based on the TCGA and GEO databases, requiring multicenter, large-sample clinical trials to validate the clinical value of the model. Additionally, our research is currently mainly based on bioinformatics analysis. In the future, we can conduct *in vivo* and *in vitro* experiments to further verify the research results. For example, culturing LUAD cell lines and normal lung epithelial cells for subsequent *in vitro* experiments will enable us to more directly observe the functional role of RMlncRNAs in LC cells; using small interfering RNA (siRNA) or plasmid technology to conduct gene knockdown or overexpression studies on identified RMlncRNAs; using quantitative real-time polymerase chain reaction (qRT-PCR) and western blot analysis techniques to verify the expression level of RMlncRNAs and their interaction with target proteins, which will provide us with important clues to reveal the molecular mechanism of RMlncRNAs in the occurrence and development of LC; constructing mouse models (such as xenograft models) injected with LUAD cell lines manipulated by RMlncRNAs for *in vivo* experimental studies. This will enable us to observe the functional role of RMlncRNAs in an environment closer to the human body and provide strong support for its development as a potential therapeutic target.

Conclusions

In this study, 18 RMlncRNAs associated with prognosis in LUAD patients were analyzed to establish a risk model with good reliability in predicting patient survival, and to reveal the correlation between immune characteristics and chemotherapy drug sensitivity in LUAD patients. This can provide important guidance for personalized treatment of clinical LUAD patients, and promote the development of tumor therapy.

Acknowledgments

The authors thank the TCGA dataset and GEO dataset for providing high quality data.

Footnote

Reporting Checklist: The authors have completed the TRIPOD reporting checklist. Available at https://tcr.amegroups.com/article/view/10.21037/tcr-24-1085/rc

Peer Review File: Available at https://tcr.amegroups.com/article/view/10.21037/tcr-24-1085/prf

Funding: This work was supported by the Yunnan Fundamental Research Projects (Nos. 202301AT070094, 202201AT070380); and the Joint Special Funds for the Department of Science and Technology of Yunnan Province-Kunming Medical University (No. 202201AY070001-156).

Conflicts of Interest: All authors have completed the ICMJE uniform disclosure form (available at https://tcr.amegroups.com/article/view/10.21037/tcr-24-1085/coif). The authors

have no conflicts of interest to declare.

Ethical Statement: The authors are accountable for all aspects of the work in ensuring that questions related to the accuracy or integrity of any part of the work are appropriately investigated and resolved. The study was conducted in accordance with the Declaration of Helsinki (as revised in 2013).

References

1. Sung H, Ferlay J, Siegel RL, et al. Global Cancer Statistics 2020: GLOBOCAN Estimates of Incidence and Mortality Worldwide for 36 Cancers in 185 Countries. CA Cancer J Clin 2021;71:209-49.
2. Woodman C, Vundu G, George A, et al. Applications and strategies in nanodiagnosis and nanotherapy in lung cancer. Semin Cancer Biol 2021;69:349-64.
3. Li Y, Liu Y, Wang K, et al. STK24 Promotes Progression of LUAD and Modulates the Immune Microenvironment. Mediators Inflamm 2023;2023:8646088.
4. Liu Y, Zhang H, Zhang W, et al. circ_0004140 promotes LUAD tumor progression and immune resistance through circ_0004140/miR-1184/CCL22 axis. Cell Death Discov 2022;8:181.
5. Dantoing E, Piton N, Salaün M, et al. Anti-PD1/PD-L1 Immunotherapy for Non-Small Cell Lung Cancer with Actionable Oncogenic Driver Mutations. Int J Mol Sci 2021;22:6288.
6. Tsuboi M, Herbst RS, John T, et al. Overall Survival with Osimertinib in Resected EGFR-Mutated NSCLC. N Engl J Med 2023;389:137-47.
7. Torre LA, Siegel RL, Jemal A. Lung Cancer Statistics. Adv Exp Med Biol 2016;893:1-19.
8. Xu Y, Zhang M, Zhang Q, et al. Role of Main RNA Methylation in Hepatocellular Carcinoma: N6-Methyladenosine, 5-Methylcytosine, and N1-Methyladenosine. Front Cell Dev Biol 2021;9:767668.
9. Xie S, Chen W, Chen K, et al. Emerging roles of RNA methylation in gastrointestinal cancers. Cancer Cell Int 2020;20:585.
10. Liu Q, Gregory RI. RNAmod: an integrated system for the annotation of mRNA modifications. Nucleic Acids Res 2019;47:W548-55.
11. Zhang C, Zhang M, Ge S, et al. Reduced m6A modification predicts malignant phenotypes and augmented Wnt/PI3K-Akt signaling in gastric cancer. Cancer Med 2019;8:4766-81.
12. An Y, Duan H. The role of m6A RNA methylation in cancer metabolism. Mol Cancer 2022;21:14.
13. Wang Q, Chen C, Ding Q, et al. METTL3-mediated m(6)A modification of HDGF mRNA promotes gastric cancer progression and has prognostic significance. Gut 2020;69:1193-205.
14. Chen M, Wei L, Law CT, et al. RNA N6-methyladenosine methyltransferase-like 3 promotes liver cancer progression through YTHDF2-dependent posttranscriptional silencing of SOCS2. Hepatology 2018;67:2254-70.
15. Li T, Hu PS, Zuo Z, et al. METTL3 facilitates tumor progression via an m(6)A-IGF2BP2-dependent mechanism in colorectal carcinoma. Mol Cancer 2019;18:112.
16. Pan J, Huang Z, Xu Y. m5C RNA Methylation Regulators Predict Prognosis and Regulate the Immune Microenvironment in Lung Squamous Cell Carcinoma. Front Oncol 2021;11:657466.
17. Zhang Q, Liu F, Chen W, et al. The role of RNA m(5) C modification in cancer metastasis. Int J Biol Sci 2021;17:3369-80.
18. Ma JZ, Yang F, Zhou CC, et al. METTL14 suppresses the metastatic potential of hepatocellular carcinoma by modulating N(6) -methyladenosine-dependent primary MicroRNA processing. Hepatology 2017;65:529-43.
19. Han M, Huang Q, Li X, et al. M7G-related tumor immunity: novel insights of RNA modification and potential therapeutic targets. Int J Biol Sci 2024;20:1238-55.
20. Zhang X, Zhu WY, Shen SY, et al. Biological roles of RNA m7G modification and its implications in cancer. Biol Direct 2023;18:58.
21. Ma J, Han H, Huang Y, et al. METTL1/WDR4-mediated m(7)G tRNA modifications and m(7)G codon usage promote mRNA translation and lung cancer progression. Mol Ther 2021;29:3422-35.
22. Jathar S, Kumar V, Srivastava J, et al. Technological Developments in lncRNA Biology. Adv Exp Med Biol 2017;1008:283-323.
23. Sun Z, Xue S, Zhang M, et al. Aberrant NSUN2-

mediated m(5)C modification of H19 lncRNA is associated with poor differentiation of hepatocellular carcinoma. Oncogene 2020;39:6906-19.
24. Fang D, Ou X, Sun K, et al. m6A modification-mediated lncRNA TP53TG1 inhibits gastric cancer progression by regulating CIP2A stability. Cancer Sci 2022;113:4135-50.
25. Dong K, Gu D, Shi J, et al. Identification and Verification of m(7)G Modification Patterns and Characterization of Tumor Microenvironment Infiltration via Multi-Omics Analysis in Clear Cell Renal Cell Carcinoma. Front Immunol 2022;13:874792.
26. Hu BB, Wang XY, Gu XY, et al. N(6)-methyladenosine (m(6)A) RNA modification in gastrointestinal tract cancers: roles, mechanisms, and applications. Mol Cancer 2019;18:178.
27. Li Y, Xiao J, Bai J, et al. Molecular characterization and clinical relevance of m(6)A regulators across 33 cancer types. Mol Cancer 2019;18:137.
28. Meng L, Zhang Q, Huang X. Abnormal 5-methylcytosine lncRNA methylome is involved in human high-grade serous ovarian cancer. Am J Transl Res 2021;13:13625-39.
29. Song P, Tayier S, Cai Z, et al. RNA methylation in mammalian development and cancer. Cell Biol Toxicol 2021;37:811-31.
30. Colaprico A, Silva TC, Olsen C, et al. TCGAbiolinks: an R/Bioconductor package for integrative analysis of TCGA data. Nucleic Acids Res 2016;44:e71.
31. Mayakonda A, Lin DC, Assenov Y, et al. Maftools: efficient and comprehensive analysis of somatic variants in cancer. Genome Res 2018;28:1747-56.
32. Zhang H, Meltzer P, Davis S. RCircos: an R package for Circos 2D track plots. BMC Bioinformatics 2013;14:244.
33. Geeleher P, Cox N, Huang RS. pRRophetic: an R package for prediction of clinical chemotherapeutic response from tumor gene expression levels. PLoS One 2014;9:e107468.
34. Brunson JC. ggalluvial: Layered Grammar for Alluvial Plots. J Open Source Softw 2020;5:2017.
35. Hu K. Become Competent in Generating RNA-Seq Heat Maps in One Day for Novices Without Prior R Experience. Methods Mol Biol 2021;2239:269-303.
36. Thai AA, Solomon BJ, Sequist LV, et al. Lung cancer. Lancet 2021;398:535-54.
37. Chen DT, Chan W, Thompson ZJ, et al. Utilization of target lesion heterogeneity for treatment efficacy assessment in late stage lung cancer. PLoS One 2021;16:e0252041.
38. Kan RL, Chen J, Sallam T. Crosstalk between epitranscriptomic and epigenetic mechanisms in gene regulation. Trends Genet 2022;38:182-93.
39. Chen X, Liu Y, Sun D, et al. Long noncoding RNA lnc-H2AFV-1 promotes cell growth by regulating aberrant m6A RNA modification in head and neck squamous cell carcinoma. Cancer Sci 2022;113:2071-84.
40. Wanna-Udom S, Terashima M, Lyu H, et al. The m6A methyltransferase METTL3 contributes to Transforming Growth Factor-beta-induced epithelial-mesenchymal transition of lung cancer cells through the regulation of JUNB. Biochem Biophys Res Commun 2020;524:150-5.
41. Wang T, Kong S, Tao M, et al. The potential role of RNA N6-methyladenosine in Cancer progression. Mol Cancer 2020;19:88.
42. Tang LX, Chen GH, Li H, et al. Long non-coding RNA OGFRP1 regulates LYPD3 expression by sponging miR-124-3p and promotes non-small cell lung cancer progression. Biochem Biophys Res Commun 2018;505:578-85.
43. Dong H, Liu Q, Chen C, et al. LncRNA OGFRP1 promotes angiogenesis and epithelial-mesenchymal transition in colorectal cancer cells through miR-423-5p/CTCF axis. Immunobiology 2022;227:152176.
44. Zhang J, Xu X, Yin J, et al. lncRNA OGFRP1 promotes tumor progression by activating the AKT/mTOR pathway in human gastric cancer. Aging (Albany NY) 2021;13:9766-79.
45. Yang M, He X, Huang X, et al. LncRNA MIR4435-2HG-mediated upregulation of TGF-β1 promotes migration and proliferation of nonsmall cell lung cancer cells. Environ Toxicol 2020;35:582-90.
46. Zhong C, Xie Z, Zeng LH, et al. MIR4435-2HG Is a Potential Pan-Cancer Biomarker for Diagnosis and Prognosis. Front Immunol 2022;13:855078.
47. Ghasemian M, Rajabibazl M, Sahebi U, et al. Long non-coding RNA MIR4435-2HG: a key molecule in progression of cancer and non-cancerous disorders. Cancer Cell Int 2022;22:215.
48. Zhao F, Liu Y, Tan F, et al. MIR4435-2HG: A Tumor-associated Long Non-coding RNA. Curr Pharm Des 2022;28:2043-51.
49. Wei L, Liu Y, Zhang H, et al. TMPO-AS1, a Novel E2F1-Regulated lncRNA, Contributes to the Proliferation of Lung Adenocarcinoma Cells via Modulating miR-326/SOX12 Axis. Cancer Manag Res 2020;12:12403-14.
50. Li Q, Bian Y, Li Q. Down-Regulation of TMPO-AS1 Induces Apoptosis in Lung Carcinoma Cells by Regulating miR-143-3p/CDK1 Axis. Technol Cancer Res Treat 2021;20:1533033820948880.
51. Pandini C, Pagani G, Tassinari M, et al. The pancancer

overexpressed NFYC Antisense 1 controls cell cycle mitotic progression through in cis and in trans modes of action. Cell Death Dis 2024;15:206.
52. Song Y, Du J, Lu P, et al. LncRNA NFYC-AS1 promotes the development of lung adenocarcinomas through autophagy, apoptosis, and MET/c-Myc oncogenic proteins. Ann Transl Med 2021;9:1621.
53. Tong F, Xu L, Xu S, et al. Identification of an autophagy-related 12-lncRNA signature and evaluation of NFYC-AS1 as a pro-cancer factor in lung adenocarcinoma. Front Genet 2022;13:834935.
54. Ding Y, Huang Y, Zhang F, et al. LncRNA TDRKH-AS1 promotes breast cancer progression via the miR-134-5p/CREB1 axis. J Transl Med 2023;21:854.
55. Jiao Y, Zhou J, Jin Y, et al. Long Non-coding RNA TDRKH-AS1 Promotes Colorectal Cancer Cell Proliferation and Invasion Through the β-Catenin Activated Wnt Signaling Pathway. Front Oncol 2020;10:639.
56. Kretz M, Webster DE, Flockhart RJ, et al. Suppression of progenitor differentiation requires the long noncoding RNA ANCR. Genes Dev 2012;26:338-43.
57. Thin KZ, Liu X, Feng X, et al. LncRNA-DANCR: A valuable cancer related long non-coding RNA for human cancers. Pathol Res Pract 2018;214:801-5.
58. Lu QC, Rui ZH, Guo ZL, et al. LncRNA-DANCR contributes to lung adenocarcinoma progression by sponging miR-496 to modulate mTOR expression. J Cell Mol Med 2018;22:1527-37.
59. Wang M, Gu J, Zhang X, et al. Long Non-coding RNA DANCR in Cancer: Roles, Mechanisms, and Implications. Front Cell Dev Biol 2021;9:753706.
60. Chalmers ZR, Connelly CF, Fabrizio D, et al. Analysis of 100,000 human cancer genomes reveals the landscape of tumor mutational burden. Genome Med 2017;9:34.
61. Hellmann MD, Nathanson T, Rizvi H, et al. Genomic Features of Response to Combination Immunotherapy in Patients with Advanced Non-Small-Cell Lung Cancer. Cancer Cell 2018;33:843-852.e4.
62. Hellmann MD, Ciuleanu TE, Pluzanski A, et al. Nivolumab plus Ipilimumab in Lung Cancer with a High Tumor Mutational Burden. N Engl J Med 2018;378:2093-104.
63. Harvey RD, Adams VR, Beardslee T, et al. Afatinib for the treatment of EGFR mutation-positive NSCLC: A review of clinical findings. J Oncol Pharm Pract 2020;26:1461-74.
64. Winegarden JD, Mauer AM, Gajewski TF, et al. A phase II study of bryostatin-1 and paclitaxel in patients with advanced non-small cell lung cancer. Lung Cancer 2003;39:191-6.

Cite this article as: Zhang L, Yang L, Chen X, Huang Q, Ouyang Z, Wang R, Xiang B, Lu H, Ren W, Wang P. Construction and validation of a prognostic model of lncRNAs associated with RNA methylation in lung adenocarcinoma. Transl Cancer Res 2025;14(2):761-777. doi: 10.21037/tcr-24-1085